STUDIES OF THE CYTOCHROME c_1 SUBUNIT OF CYTOCHROME bc_1 COMPLEX FROM *RHODOBACTER SPHAEROIDES*

By

MARIA ELBERRY

Bachelor of Science

Lebanese American University

Byblos, Lebanon

2002

Submitted to the Faculty of the
Graduate College of the
Oklahoma State University
in partial fulfillment of
the requirements for the degree of
MASTERS OF SCIENCE
Dec 2005

STUDIES OF THE CYTOCHROME c_1 SUBUNIT

OF CYTOCHROME bc_1 COMPLEX FROM

RHODOBACTER SPHAEROIDES

Thesis Approved:

Chang-An Yu

Thesis Adviser

Linda Yu

Richard Essenberg

A. Gordon Emslie

Dean of the Graduate College

ACKNOWLEDGEMENTS

I intensely and deeply thank my parents, Antoine Elberry and Joumana Saber for their encouragement, moral and financial support.

I wish to express sincere gratitude to my advisor Dr. Chang-An Yu for his supervision, inspiration and encouragement throughout my graduate program. I am also equally grateful to Dr. Linda Yu for her motivation and support during my study. My sincere appreciation also extends to my graduate committee member Dr. Richard Essenberg for his assistance and guidance throughout my graduate years.

I would also like to thank Dr. Di Xia for his collaboration and support and above all for his valuable advices.

I also thank all professors and staff of the Biochemistry and Molecular Biology department and all the former and current students of Dr Yu's lab, especially Dr. Shih-Chia Tso (Scott) and Dr. Kunhung Xiao (Kevin).

TABLE OF CONTENTS

Chapter page

LIST OF FIGURES

LIST OF TABLES

Table page

NOMENCLATURE

ADP	Adenosine di-phosphate
ATP	Adenosine tri-phosphate
Asc	Ascorbate
bc_1	Ubiquinol-cytochrome *c* oxidoreductase
b_H	Higher potential cytochrome *b* heme
b_L	Lower potential cytochrome *b* heme
Cyt	Cytochrome
CO	Carbon monoxide
DNA	Deoxyribonucleic Acid
DSC	Differential scanning calorimetry
E. coli	*Escherichia coli*
EDTA	Ethylenediaminetetramethylacetic acid
Em	Midpoint potential
FAD	Flavin adenosine dinucleotide – oxidized form
$FADH_2$	Flavin adenosine dinucleotide – reduced form
HRP	horseradish peroxidase
ICM	Intracytoplasmic membrane
ISP	Iron Sulfur Protein
KDa	Kilo Daltons

Kb	Kilo Base-pairs
LB	Luria Broth
ME	Mercaptoethanol
NAD	Nicotinamide adenosine dinucleotide – oxidized form
$NADH_2$	Nicotinamide adenosine dinucleotide – reduced form
PAGE	Polyacrylamide gel electrophoresis
Pi	Inroganic phosphate
Ps.	Photosynthetic
Q	Ubiquinone
$QH^{\cdot}$	Semiubiquinol
QH_2	Ubiquinol
Qi	Inside ubiquinol site
Qo	Outside ubiquinone site
$Q_0C_{10}BrH_2$	2,3-Dimethoxy-5-methyl-6-(10-bromodecyl)-1,4-benzoquinol
Rb.	*Rhodobacter*
SDS	Sodium dodecyl sulfate
Tm	Melting temperature
TMBZ	3,3',5,5'-tetramethyl benzidine dihydrochloride
UV	Ultra Violet
[2Fe2S]	Iron sulfur cluster

CHAPTER I

INTRODUCTION

A. Mitochondrial respiratory chain

In eukaryotes, mitochondria perform several fundamental cellular functions. The major function of mitochondria is to generate energy for cellular activity through oxidative phosphorylation (Fig. 1), which is based on the sequential operation of five protein complexes, complexes I through V, four of which constitute the mitochondrial electron transfer chain; complexes I through IV. NADH and succinate, two products of the citric acid cycle, are electron donors of the electron transfer chain through complex I and complex II, respectively. Complex I, NADH-ubiquinone oxidoreductase, transfers electrons from NADH to ubiquinone. Complex II, succinate-ubiquinone oxidoreductase, transfers electrons from succinate to ubiquinone. Ubiquinol reduces complex III, ubiquinol-cytochrome *c* reductase, which transfers the electron through cytochrome *c* to complex IV, cytochrome *c* oxidase. The final electron acceptor in the electron transfer chain is oxygen. Electron transfer through these complexes, except for complex II, is coupled to proton translocation from the matrix into the inter-membrane space, establishing a proton gradient across the inner membrane. Complex V, ATP synthase, uses this transmembrane proton gradient to drive the endergonic reaction of ATP synthesis. The conversion of osmotic energy of the gradient into chemical energy, achieved by complex V, is

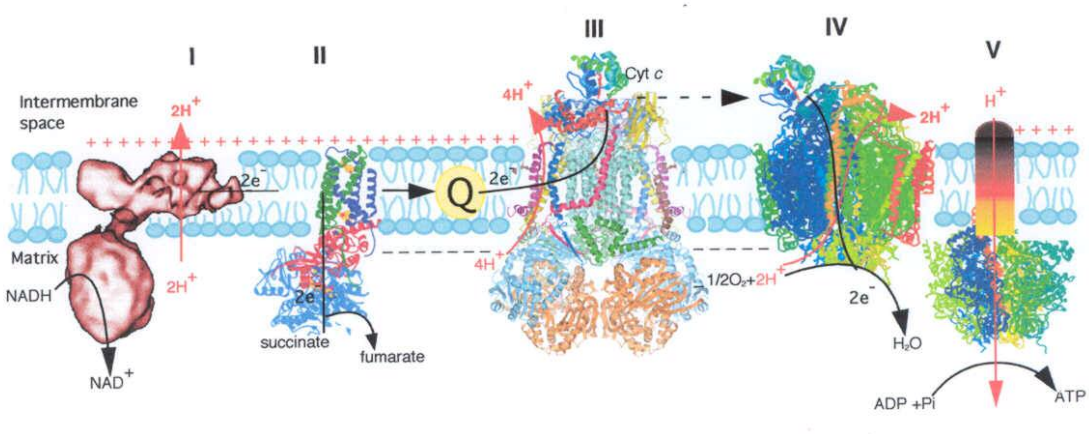

Figure 1: Mitochondrial electron transport chain complexes. Black arrows and dashed arrows illustrate proton translocation and electron transport, respectively.

known as the chemiosmotic coupling process.

In the aerobic respiratory system of bacteria, complex III, also referred to as the cytochrome bc_1 complex, perform a similar function as in the mitochondria. In chloroplasts and cyanobacteria, the bc_1 complex is substituted by a similar complex called the cytochrome b_6f or plastoquinol-plastocyanin oxidoreductase that performs the same function in the electron transfer chain. Similarity between the two complexes is high enough to believe most features discussed about one complex apply to the other.

B. The cytochrome bc_1 complex

The cytochrome bc_1 complex is a vital constituent of the electron transfer pathway of mitochondria and many respiratory and photosynthetic bacteria (1-5). It catalyzes the electron transfer from quinol to a *c*-type cytochrome with generation of a proton gradient used for ATP synthesis. All cytochrome bc_1 complexes contain three redox subunits (Table 1) housing four redox centers: cytochrome *b*, which houses two *b*-type hemes (b_L or b_{566} and b_H or b_{562}), cytochrome c_1 which houses a *c*-type heme and the Rieske iron-sulfur protein, which houses a high-potential [2Fe2S] cluster (4). Some cytochrome bc_1 complexes consist of additional supernumerary subunits that vary in number in different species (Table 1). For example, the bc_1 complex in bovine heart contains eight supernumerary subunits (6), in yeast, it contains seven (7), in *Rhodobacter sphaeroides* it has only one (8) and none in *Rhodobacter capsulatus* (9). Although the function of supernumerary subunits is still not fully understood, it is well established that complexes lacking these subunits are

(A)

Core Subunits	**Prosthetic Group**
Cytochrome *b*	Hemes b_L and b_H
Cytochrome c_1	Heme c_1
Rieske Iron Sulfur Protein	[2Fe2S] Iron Sulfur Cluster

(B)

Source	**Core Subunit**	**Supernumerary Subunit**
Bovine	3	8
Yeast	3	7
Rhodobacter sphaeroides	3	1
Rhodobacter capsulatus	3	0
Paracoccus denitrificans	3	0

Table 1: (A) The three prosthetic groups found in all cytochrome bc_1 complex.

(B) Number of core subunits and supernumerary subunits found in the cytochrome bc_1 complex from different species.

less stable and show lower enzyme activity compared to complexes with supernumerary subunits (7,10). Therefore, it is possible that increased stability and activity of the complex result from the interaction between the redox subunits and the supernumerary subunits.

C. The Q cycle mechanism

The "protonmotive Q Cycle" hypothesis, proposed by Peter Mitchell (11), explains electron transfer and proton translocation in the cytochrome bc_1 complex. Up to this date, several different opinions were projected about the mechanism through which the bc_1 complex operates but the "Q Cycle mechanism" is the generally accepted one because it fully explains the kinetics of reduction of cytochrome c_1 and heme b_H (12).

The two major features of the Q cycle mechanism (Fig. 2) are, first, the existence of two ubiquinone binding site (Qo and Qi sites) and second, the bifurcated reaction at the Qo site (13). In the first turnover of the cycle, one ubiquinol molecule (QH_2) is oxidized at the Qo site on the positive side of the inner mitochondrial membrane where the two electrons diverge with one electron transferred to the high potential chain through 2Fe2S cluster (E_m= 280mV) then heme c_1 (E_m=227mV) to cytochrome c and the second electron transferred to the low potential chain through heme b_L (E_m = -30mV) to heme b_H (E_m = 90mV) which reduces ubiquinone (Q) to ubisemiquinone ($QH^{\cdot}$) at the Qi site uptaking one proton from the matrix. In the second turnover of the cycle, the bifurcated electrons at the Qo site follow the same two paths except that heme b_H will transfer the electron to ubisemiquinone, generated in the first turnover,

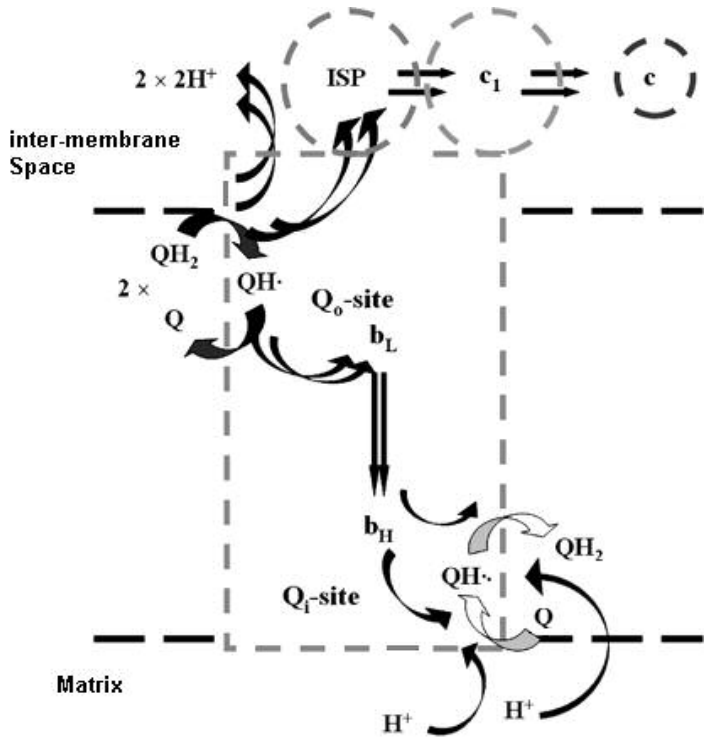

Figure 2: The Q-cycle mechanism showing the reactions catalyzed by the bc_1 complex. The first turnover of the cycle follows the arrow labeled "1" reducing ubiquinone (Q) to ubisemiquinone ($QH^{\cdot}$) and the second turnover of the cycle follows the arrow labeled "2" reducing ubisemiquinone ($QH^{\cdot}$) to ubiquinol (QH_2).

and reduce it to ubiquinol (QH_2), with the uptake of another proton from the matrix. Therefore, in a complete turnover of the cytochrome bc_1 complex, as pointed out in the equation below, one quinone molecule is generated, two cytochrome *c* molecules are reduced and four protons are deposited in the intermembrane space; two protons are deposited upon oxidation of one QH_2 molecule at the Qo site.

$$QH_2 + 2 \text{ cyt } c^{3+} + 2H^+_{(in)} \Rightarrow Q + 2 \text{ cyt } c^{2+} + 4H^+_{(out)}$$

D. The three dimensional structure of the cytochrome bc_1 complex

The three-dimensional structure of the cytochrome bc_1 complex from bovine heart mitochondria, chicken and yeast were determined by X-ray crystallography at a resolution of 2.4 Å (14) , 3.16 Å (15) and 2.3 Å (16), respectively . The bovine structure (Fig. 3) is the most complex one composed of three redox subunits and eleven supernumerary subunits, which fold into a pear-shaped dimeric structure of 130 Å width and 155 Å height. The complex lengthens 38 Å in the intermembrane space from the inner membrane surface housing cytochrome c_1 head and ISP head as well as subunit VIII. The complex extends 42 Å through the inner membrane consisting of five transmembrane helices from cytochrome b and one helix from each of cytochrome c_1, ISP, subunits VII, X and XI. In the matrix region, the complex extends 75 Å and consists of CoreI and CoreII subunits, subunits VI and IX as well the C-terminal fragment of ISP and the N-terminal fragment of subunit VII (17). The structural features of the bc_1 complex help understand the mechanism of function of the complex. So far, all structural data support the Q-cycle mechanism, the existence of the bc_1 complex in an intertwined dimeric conformation and the essentiality of the

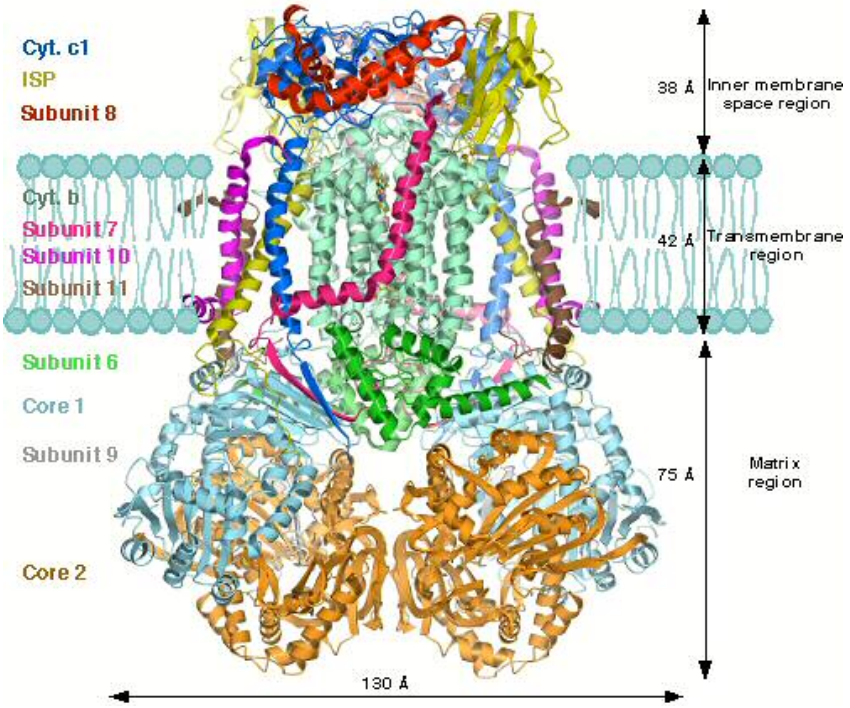

Figure 3. The intertwined dimeric structure of bovine cytochrome bc_1 complex

head domain movement of ISP for bc_1 catalysis.

1. The intertwined dimeric structure of the bc_1 complex

Crystallographic observations suggest that the bc_1 complex exists and functions as a dimer with the ISPs of the two monomers intertwined as the ISP tail folds in one monomer and its head domain is in close proximity with cyt *b* and cyt c_1 of the other monomer. To further confirm this observation, mutant bc_1 complexes were generated where two disulfide bonds were introduced between ISP and cyt *b*, one between the head domain of ISP and cyt *b* and the other one between the tail domain of ISP and cyt *b*. SDS-PAGE analysis of this mutant, which shows an adduct protein of molecular weight 128KDa consisting of two cyt *b* subunits and two ISP subunits, confirm that the bc_1 complex exists as a dimer with intertwining ISPs (18).

The functional significance of the dimeric structure of the complex was also implied by studying electron transfer between the two heme b_Ls of the bc_1 complex. The distance between the two heme b_Ls is short enough (21 Å) to allow this transfer and recent studies revealed that disruption of electron transfer between the two b_L hemes increases electron leakage to oxygen resulting in decreased ubiquinol-cytochrome *c* reductase activity (19).

2. Head domain movement of ISP

As revealed by the structure, ISP tail domain (N-terminal) spans the inner membrane and its neck and head domain (C-terminal) are located in the intermembrane space. The head domain movement of ISP between Qo site and cyt c_1

of about 22 Å is presumed critical in the bifurcation of the electron pathway (15). The head domain movement of ISP was further supported by the observation of different [2Fe-2S] cluster positions using different types of Qo inhibitors which either fix ISP head domain in cyt *b* position or leave ISP head domain mobile (20-22). Moreover, several studies were done on a molecular level confirming the crucial role of the head movement in bc_1 catalysis. By increasing the rigidity of the neck domain of ISP by amino acid substitution to Proline (23) or by introducing a disulfide bond in the neck region (24), which decreases the flexibility of the head domain, the enzymatic activity of the bc_1 complex was decreased. In the latter case, activity can be restored only by reducing the disulfide bond. Moreover, a disulfide bond was introduced between the head domain of ISP and cytochrome *b* to completely immobilize the head domain in the *b*-position. Formation of the inter-subunit disulfide bond completely abolishes the cytochrome bc_1 activity which can be restored to normal activity by reducing the disulfide bond with β-mercaptoethanol (25).

The ISP head domain movement hypothesis may also explain the bifurcated reaction at the Qo site. When quinol is oxidized at the Qo site, one electron is passed to the high potential chain through [2Fe-2S] cluster and the second electron is passed to the low potential chain through heme b_L. The latter thermodynamically unfavorable process could be explained by the head domain movement of ISP; in one model, when the first electron is passed to the iron-sulfur cluster of ISP, ISP head is held in the *b*-position. The iron sulfur cluster being reduced, it cannot accept another electron and only after the second electron is passed to the low potential chain, ISP head moves toward cyt c_1 (26-27). In a different model, proposed by Xiao et. al. (18),

ISP head is held in the c_1-position, too far from the Qo site for the second electron to be transferred to it, until the second electron is passed to heme b_L.

All features of bovine bc_1 complex discussed above also apply to the *Rhodobacter sphaeroides* bc_1 complex, which was used as the study system in this thesis.

E. Photosynthetic bacterium *Rhodobacter sphaeroides* cytochrome bc_1 complex

The photosynthetic bacterium *Rb. sphaeroides* is an anoxygenic purple bacterium that carries out photosynthesis under anaerobic conditions without producing oxygen, in contrast to plants and algae. *Rb. sphaeroides* can also grow under aerobic conditions in the dark when cytochrome bc_1 complex is dispensable for the bacterium growth. Therefore, mutated bc_1 complex that cannot support photosynthetic cell growth can still be purified. In photosynthetic growth under anaerobic conditions, the cyt bc_1 complex is required for bacterial growth to transfer electrons from quinol to cytochrome c_2. If the cyt bc_1 complex is defective and cannot support photosynthetic growth, cells can be grown under semi-aerobic conditions in the dark where the cyt bc_1 complex is not required because of the presence of quinol oxidase, which transfers the electron directly to oxygen in a cyt bc_1-independent pathway. Under these conditions, intracytoplasmic membrane (ICM) is synthesized from which defective cyt bc_1 complex can be purified and characterized. The ability of *Rb. sphaeroides* to grow under semi-aerobic and anerobic conditions, synthesizing cyt bc_1 complex under either condition, makes it an ideal system for the study of the cyt bc_1 complex. Besides, the bacterial cyt bc_1 complex is a simple protein composed

of only four subunits, three catalytic subunits (cyto *b*, cyt c_1 and ISP) similar to their bovine counterparts and one supernumerary subunit, subunit IV. All subunits are encoded by genes organized in an *fbc*FBCQ operon, which was deleted from the chromosome of *Rb. sphaeroides* to facilitate mutagenesis studies. Each of cyt *b*, cyt c_1, ISP and subunit IV of the cyt bc_1 complex can be characterized individually using molecular and biochemical techniques to further visualize the structure of the subunit and understand its function in cyt bc_1 complex catalytic activity. This study focuses on cyt c_1 subunit of *Rb. sphaeroides* cyt bc_1 complex. Several mutagenic and biochemical techniques are used to depict new structural and functional features of *Rb. sphaeroides* cyt c_1 that cannot be envisioned in the bovine structure of the bc_1 complex.

F. Cytochrome c_1 subunit

Mitochondrial cytochrome c_1 was discovered in 1940 by two independent groups, Yakushiji & Okunaki (28) and Keilin & Hartree (29) and its sequence was determined in 1980 by Wakabayashi *et. al.* (30). It consists of 241 residues and is synthesized as a precursor with a leading sequence of around 80 residues (31). Cytochrome c_1 folds in a similar way to cytochrome *c* and other class I cytochromes with some insertions and deletions in different linker peptides between the core helices. Cytochrome c_1 assembles into an extrinsic hydrophilic domain anchored to the membrane through a C-terminal hydrophobic transmembrane α-helice.

Rhodobacter sphaeroides cytochrome c_1 is composed of 263 amino acids but is synthesized as a precursor with 285 amino acids (32) and has a theoretical

molecular mass of 30.5KDa but is identified as a protein with a molecular weight of 34KDa on SDS-PAGE. In overloaded samples, cytochrome c_1 can be identified on gels by the color of the covalently bound heme or by the peroxidase activity of the heme.

Mature *Rb. sphaeroides* cytochrome c_1 houses a type c heme and contains the conserved CXXCH heme-binding consensus sequence in the head domain, located 37 residues downstream of the N-terminus that covalently binds the heme group through the two cysteins Cys37 and Cys40. The fifth axial ligand to the heme iron is His41 and the sixth axial ligand is a conserved methionine located at residue 185, close to the C-terminus end. Sequence alignment between bovine and *Rb. sphaeroides* cyt c_1 reveals two fragment insertions in the bacterial cyt c_1; the first 17-amino acid fragment extends from residue Gly109 to Ile125 located downstream of the conserved PDL sequence and the second 19-amino acid fragment extends from residue Gln161 to Ala179 located upstream of the sixth ligand to the heme, Met185. These insertions are absent in cytochromes c_1 of higher organisms such as bovine and yeast but are present in *Rb. capsulatus* and *Rb. sphaeroides*. The second extra fragment includes a cystein at residue 169 that aligns with Cys167 of *Rb. capsulatus*. Another cystein residue is located at residue 145 in *Rb. sphaeroides* that aligns with Cys144 in *Rb. capsulatus*. Because the two cysteins are absent in cyt c_1 sequence of higher organisms, such as bovine, chicken and yeast, whose crystal structure was solved (16, 33-36), no structural data can assert the orientation and state of the cystein residues in native *Rb. sphaeroides* bc_1 complex.

G. Purpose of study

Recently, Ozyczka, A et. al. (37) reported that the two cysteins in *Rb. capsulatus* cyt c_1 form a disulfide bridge. When the bridge is disrupted, a second site suppression mutation of Ala181 to a β-branched amino acid (Thr or Val) spontaneously occur and the functionality of the cytochrome bc_1 complex is restored. This mutation was found to be located two residues away (βXM) from the sixth axial ligand to the heme, Met183. The presence of either the disulfide bond or the βXM residue was found to be sufficient to maintain an active cytochrome bc_1 complex. When cysteins were mutated to alanine and a β-branched amino acid was inserted at βXM position, the redox potential of *Rb. capsulatus* cyt c_1 was lowered from 320mV to 227mV, which is comparable to that of wild type *Rb. sphaeroides* cyt c_1. This would suggest that *Rb. sphaeroides* cyt c_1 which has comparable properties, a β-branched amino acid (Ile) at position βXM and a redox potential of 230mV, does not have a disulfide bond. The presence of a disulfide bond in *Rb. capsulatus* cyt c_1 was confirmed by the crystal structure data of the *Rb. capsulatus* cyt bc_1 complex at 3.8Å (38).

Herein, we investigate the state of the cysteins in *Rb. sphaeroides* cyt c_1 using genetic and biochemical techniques. The photosynthetic growth behavior, cyt bc_1 complex activity and stability and redox potential of cyt c_1 in purified complex from wild type and mutant strains were determined and examined. Factor Xa catalysis was performed and analyzed by SDS-PAGE and Western blot. All results reveal that the two non-heme binding cysteins are connected through a disulfide bridge. We believe that when the bridge is disrupted, the second extra fragment loop (Gln161-Ala179) which includes one of the cysteins is released resulting in fluctuation of the loop. This

structural alteration results in a change in the functionality of cyt c_1 and the stability of the cyt bc_1 complex.

CHAPTER II

MATERIALS AND METHODS

A. Materials

Cytochrome c (from horse heart) and TMBZ (3, 3', 5, 5'-tetramethyl benzidine dihydrochloride) were purchased from Sigma. N-Dodecyl-*β*-D-maltoside (LM) and N-octyl-β-D-glucoside (OG) were from Anatrace. Ni-NTA gel and Qiaprep Spin Miniprep Kit were from Qiagen. 2, 3-Dimethoxy-5-methyl-6-(10-bromodecyl)-1, 4-benzoquinol ($Q_0C_{10}BrH_2$) was prepared in our lab as previously reported (39). Bovine Heart cyt c_1 was purified according to the previously published method (40).

B. Methods

1. Growth of Bacteria:

E. coli cells were grown at 37ºC in LB medium. *Rhodobacter sphaeroides* BC17 cells bearing pRKD*fbc*FBC$_{6H}$Q (41) plasmid containing the *fbc* genes were grown photosynthetically at 30ºC in an enriched Sistrom medium containing 5mM glutamate and 0.2% casamino acids. Photosynthetic growth conditions for *Rb sphaeroides* were essentially as described previously (42). Antibiotics were added to the following concentrations: 125μg/mL ampicillin, 40μg/mL Kanamycin sulfate, 10μg/mL tetracycline for *E. coli* and 1μg/mL for *Rb. sphaeroides*, 100μg/mL trimethoprim

for *E. coli* and 30μg/mL for *R. sphaeroides*.

2. Generation of *Rb. Sphaeroides* expressing mutants of bc_1 complex:

Mutations were constructed by site-directed mutagenesis using the QuickChange system from Stratagene. The double stranded pGEMC_{6H}Q was used as template. pGEMC_{6H}Q was constructed by ligating the XbaI-HindIII fragment of pRKD*fbc*FBC_{6H}Q (41) into the XbaI-HindIII digested pGEM7Zf(+). The following primers were used to introduce single mutations in cyt c_1

C145A primer:

5'GGCTCATGGCCTTCGGCGGCTTTCGGCGGCTCTTCCG 3'

C169A primer:

5'CGCCGTTCGCGTCCTTGGCGGTGTCGGGGACCG 3'

C145S primer:

5'CGGTCCCCGACACCAGCAAGGACGCGAAC 3'

C169S primer: 5'GTTCGCGTCCTTGCTGGTGTCGGGGACCG 3'

A template with double mutation C145S/C169S was constructed using pGEM/C_{6H}Q with a single mutation at C145S as template and C169S primers. A similar method was used to construct C145A/C169A.

The following primer were used to introduce Factor Xa cleavage site

P151I/F154R primer:

5'GCCGAAGGCCATGAGATCGACGGCAGGTACTACAACCGCGCCTTC 3'

The presence of mutations on cyt c_1 was confirmed by DNA sequencing which was carried out at the Recombinant DNA/Protein Core Facility at Oklahoma State

University. Plasmid bearing successful mutations on cyt c_1 (C^*) was digested with XbaI and HindIII and the $C^*_{6H}Q$ bearing fragment was purified and ligated to the pRKD*fbc*FB vector, generated from digestion of pKD*fbc*$FBC_{6H}Q$ plasmid with XbaI and HindIII. The generated pRKD*fbc*$FBC^*_{6H}Q$ plasmid was chemically transformed to *E. coli* S17 cells. A plate mating procedure (41) was then used to mobilize the plasmid from *E. coli* S17 into *Rb. sphaeroides* BC17.

3. Purification of cyt bc_1 complex from *Rb. sphaeroides*

Chromatophore membranes were prepared as described previously (23) and stored at -80º C in the presence of 20% glycerol until use. Frozen chromatophores were used to prepare cyt bc_1 complex and stored at – 80º C in the presence of 10% glycerol as decribed by Tian *et al* (23)

Protein concentration was determined based on absorbance at 280nm using a converting factor of 1 $O.D_{280}$ = 0.56 mg/mL.cm. Cyt *b* (43) and cyt c_1 (44) concentrations were determined spectrophotometrically as published previously.

4. Activity assay of purified bc_1 complex

To assay the activity of cyt bc_1 complex in chromatophore membrane or intracytoplasmic membrane or in purified protein, the preparations were diluted to a final cytochrome *b* concentration of 3 μM with 50mM Tris-Cl, pH 8.0, containing 200mM NaCl and 0.01%LM. Aliqouts of 2, 4 or 6 μL of the diluted sample was added to 1 mL of assay mixture containing 0.3mM EDTA, and 100 μM cyt *c* in 100mM Na^+/K^+ phosphate buffer, pH 7.4. The assays were started by addition of 25

μM Q_2H_2. Activity was determined by measuring the reduction of cyt *c*, which is monitored by the increase in absorbance at 550 nm in a Shimadzu UV 2102 PC spectrophotometer at 23ºC, using a millimolar extinction coefficient of 18.5. For calculation purposes, the non-enzymatic oxidation of Q_2H_2 in the absence of enzyme under these conditions was subtracted.

5. Gel electrophoresis and Western Blot preparation and TMBZ heme staining

Sodium dodecyl sulfate - polyacrylamide gel electrophoresis (SDS-PAGE) was performed according to Laemmle (45) using Bio-Rad Mini Protean dual slab vertical cell. Samples were digested with 10mM Tris-Cl buffer, pH 6.8 containing 1% SDS and 3% glycerol in the presence or absence of 0.4% β-mercaptoethanol for 15 min at 23ºC or 5 min at 60ºC before being subjected to electrophoresis.

Western blot was performed with rabbit monoclonal antibodies against cyt c_1 or against His-tag. The polypeptides separated by SDS-PAGE were transferred to a polyvinylidene difluoride membrane for immunoblotting. Goat anti-rabbit IgG conjugated to alkaline phosphatase or protein A conjugated to horseradish peroxidase (HRP) was used as second antibody. Color development was done using HRP color development solution.

For TMBZ heme staining, 35mL of 0.25M sodium acetate (pH 5.0) were mixed with 15mL of freshly prepared solution of 6.3mM TMBZ and added to the blotted membrane. The membrane was incubated shaking for 45min followed by the addition of 1.1mL 30% hydrogen peroxide. Color development was observed within 5-15min.

6. Carbon monoxide binding experiment

Carbon monoxide (CO) binding experiment was performed at room temperature. Fully oxidized purified protein (2.5μM), dissolved in 100mM Tris-HCl (pH 8.0) containing 100mM NaCl, was first reduced with dithionite and the spectrum was recorded (specR), followed by a short bubbling with carbon monoxide which spectra was also recorded (specR+CO). Carbon monoxide binding was analyzed based on specCO calculation which was calculated from (specR+CO *minus* specR) spectra. No spectral change is expected if no binding of CO is taking place.

7. Differential scanning calorimetry

The experiment was performed using N-DSCII machine. Purified protein (0.55mL of 15μM cyt bc_1 complex) was first degassed at room temperature for 10 min. Thermoscans from 10 to 90ºC at a rate of 1ºC/min and 2ºC/min were performed during the heating and cooling scans, respectively. Three scans were recorded, heating-cooling-heating, using the third scan as the baseline for the first scan. CpCalc program was used to calculate Tm values of purified proteins.

8. Determination of redox potential of cyt c_1 in wild type and mutant bc_1 complex

The potentiometric titrations of cyt c_1 were essentially done according to the previously published method (46, 47) using the following redox mediators (final concentration): diaminodurol (70μM), duroquinone (50μM), Pyocyanine (25μM), Anthroquinone-2-sulfonic acid (25μM), Indigo carmine (25μM), 1,2-naphthoquinone

(25μM), 1,4-benzoquinone (20μM) phenazine ethosulfate (20μM), phenazine methosulfate (20μM). Reductive potentiometric titrations were carried out using dithionite to reduce the ferricyanide oxidized sample and ferricyanide was used for oxidative titration of dithionite reduced sample. All titrations were performed at room temperature using a sealed anaerobic cuvette constantly flushed with argon. The midpoint potential of cyt c_1 was calculated by fitting the redox titration data obtained to the Nernst equation for n = 1.

9. Factor Xa proteolysis

The experiment was done based on a previously reported technique (37) with some minor modifications. The digestion was done using 150 nmoles of purified cyt bc_1 complex in 50mM Tris-Cl, pH 8.0 containing 100mM NaCl and 0.01% SDS. The sample was incubated at 50ºC for 10 min. Factor Xa was then added, to a final concentration of 1% of total protein content, and the sample with the enzyme was incubated at room temperature for 16 hours. Afterwards, loading dye was added and the sample was incubated at 23ºC for 15min before applying to SDS-PAGE.

CHAPTER III

RESULTS AND DISCUSSION

A. *Rhodobacter sphaeroides* cytochrome c_1 sensitivity to reducing agent in SDS gel electrophoresis

SDS gel electrophoresis of *Rb. sphaeroides* cyt c_1 shows sensitivity to reducing agent, unlike the other three subunits cytochrome *b*, ISP and Subunit IX (30). Under reducing conditions, cyt c_1 band shows as a sharp band whereas under non-reducing conditions it shows as a smear band. It was believed that sensitivity to reducing agent is associated with the presence of a disulfide bridge in the head domain of cyt c_1 between the two non-heme binding cysteins (22, 48) but results presented herein show that in the absence of a potential disulfide bond, cyt c_1 still shows as a smear band under non-reducing conditions. Both non-heme binding cysteins, C145 and C169 were mutated mutually to alanine and serine to prevent the formation of a disulfide bridge. Cytochrome bc_1 complexes purified from mutants were run on SDS-PAGE under reducing and non-reducing conditions. In each of the double mutants of cysteins to alanines (C145A/C169A) and cysteins to serines (C145S/C169S), cyt c_1 shows as a sharp band under reducing conditions and as a smear band under non-reducing conditions (Fig. 4). These results contradict the previously suggested hypothesis and confirm that the sensitivity of cyt c_1 to reducing agent is not related to

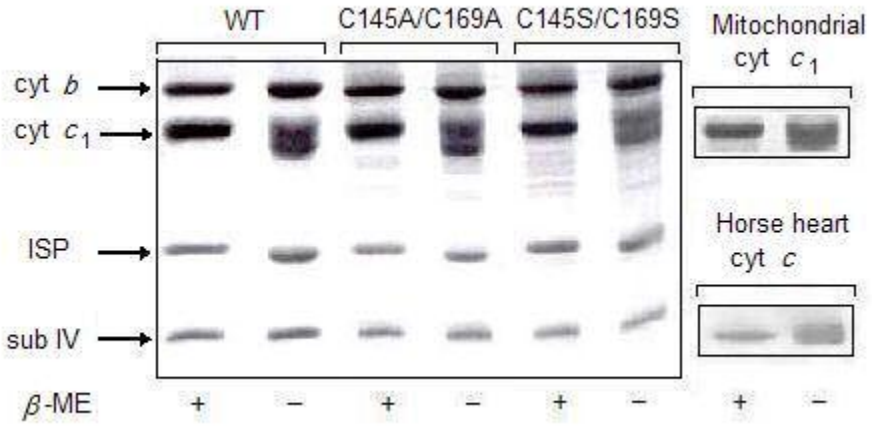

Figure 4: SDS-PAGE analysis of the cyt bc_1 complexes isolated from wild type and cystein mutants and of bovine heart mitochondrial cyt c_1 and horse heart cyt c. Samples of protein (75pmoles) were incubated under reducing (+ β-ME) or non-reducing conditions (- β-ME) at 60ºC for 5min. Cytochrome c_1 band shows as a sharp band under reducing conditions and a smeared band under non-reducing conditions in each of samples.

the presence of a disulfide bond. To examine whether such behavior is observed with *Rb. sphaeroides* cyt c_1 only or with other *c*-type cytochromes as well, horse heart cyt *c* and bovine heart mitochondrial cyt c_1 were run on SDS-page under reducing and non-reducing conditions (Fig. 4). Results show that both type *c* cytochromes are also sensitive to the presence of reducing agent. Both type *c*-cytochromes show as a sharp band and as a smear band in the presence and absence of β-mercaptoethanol, respectively. However, *Rb. capsulatus* cyt c_1, which contains a disulfide bridge between the non-heme binding cysteins, shows no such sensitivity and appears as a sharp band under reducing and non-reducing conditions (37). The reason for *Rb. capsulatus* cyt c_1 not to show as a smear band under non-reducing conditions (37) is most likely due to the small amount of sample used, because when a small amount of horse cyt *c* and larger wells are used less smear band is observed. Although no explanation for the sensitivity of heme-containing protein to reducing agent can be drawn from these results, it is obvious that the sensitivity of cyt c_1 to the presence or absence of reducing agent is not associated with the presence or absence of disulfide bond(s), since neither horse heart cyt *c* (49) nor bovine heart mitochondrial cyt c_1 (22, 50), have a disulfide bond. More experiments will be done to reveal the structural characteristic(s) that affect the mobility of c- type cytochrome polypeptides under non-reducing conditions.

B. Analysis of cystein mutants in cytochrome c_1

The non-heme binding cysteins residues in cyt c_1, C145 and C169, were mutated to alanine individually to generate the mutants C145A and C169A and mutually to

Strain	Ps. Growth	Enzymatic activity	Tm (ºC)	Cyt c_1 CO binding
Wild Type	+++	2.5	45.2	-
C145A	++	2.0	42.4	-
C169A	++	2.0	42.2	-
C145A/C169A	++	2.0	41.9	-
C145S	+	1.5	41.1	-
C169S	+	1.5	41.4	-
C145S/C169S	+	1.5	41.8	-

Table 2: Characteristics of wild type and mutants' cytochrome c_1 of the cytochrome bc_1 complex. Enzyme activity (specific activity) is expressed as μmol cyt c_{red}/min/nmoles cyt *b*. Ps. (++) and (+) refer to a photosynthetic growth rate delayed by 24hrs and 36hrs, respectively, as compared to wild type photosynthetic growth rate (+++). Methods used to calculate enzymatic activity, Tm and CO binding are described in Materials and Methods section. The data presented are mean values from three experiments.

generate the double mutant C145A/C169A. Mutants' characteristics, summarized in Table 2, reveal that mutating cystein to alanine does not severely affect the cyt bc_1 activity. About 80% of wild type activity is retained in each of the single mutants and the double mutant. Mutants can still grow photosynthetically but with a delay of 24 hours. These results suggest that the cysteins might be connected through a disulfide bridge since mutating one or both cysteins disrupt the disulfide bridge and have the same effect on mutant growth and mutant bc_1 complex activity. One way to examine the structural importance of potential free cysteins is to mutate each and both cysteins to serine and generate the single mutants C145S and C169S and the double mutant C145S/C169S. Serine mutants also grow photosynthetically but with a delay of 36 hours as compared to wild type and only 60% of wild type activity is retained, which is lower than alanine mutants activity. These results also imply that the cysteins are linked with a disulfide bridge in native protein and disruption of the bridge and insertion of two hydroxyl groups results in additional defect which results in lower protein activity. All purified mutants' complexes were subject to SDS-PAGE analysis and no difference was observed as compared to wild type; all mutants' complexes contain all four subunits with comparable intensity with the heme group covalently bound to cyt c_1, detected by TMBZ heme staining (Fig. 5).

Differential scanning calorimetry was used to check the stability of the mutant proteins. The melting temperature (Tm) of mutants' cytochrome bc_1 complexes were found to be 2.8 to 4.1ºC lower than that of wild type bc_1 complex (Table 2) which suggests that the disulfide bridge is required to maintain protein stability. Lower activity and stability of the bc_1 complex might be associated with a change in the

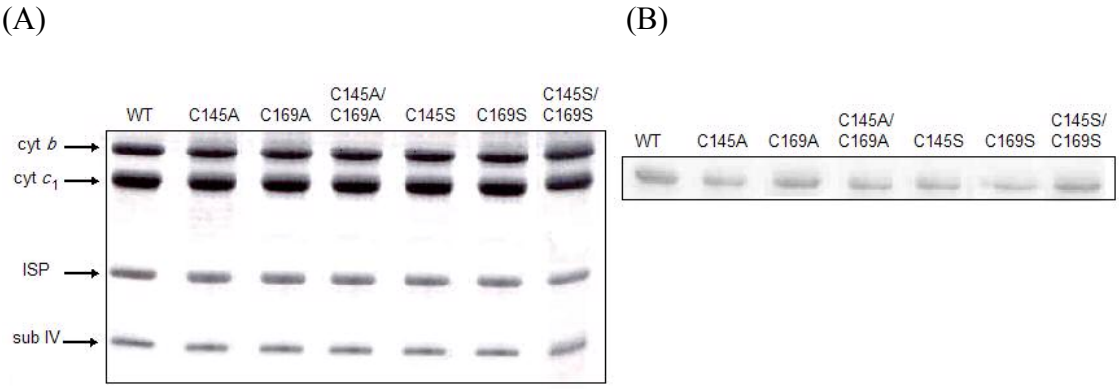

Figure 5: (A) SDS-PAGE and (B) TMBZ heme staining analysis of the cyt bc_1 complexes isolated from wild type and cystein mutants. Samples of protein (70pmoles) were incubated in the presence of β-mercaptoethanol as reducing agent at room temperature for 15min.

heme environment of cyt c_1 caused by the disruption of the disulfide bond. To examine if any of the heme ligands of cyt c_1 was altered by eliminating the disulfide bridge, we tested the ability of the mutant proteins to bind carbon monoxide. The difference spectra of (dithionite reduced + CO) *minus* (dithionite reduced) of mutated bc_1 complex were recorded and were found to be comparable to wild type profile (Fig. 6), which indicate that the ligands of heme c_1 are not affected by the disruption of the disulfide bond.

Since *Rb. sphaeroides* and *Rb. capsulatus* cyt c_1 are closely related and structurally comparable due to the high percentage of identity between the sequences, solving the structure of *Rb. capsulatus* cyt bc_1 complex (38) and of cyt c_1 head domain specifically (Fig. 7) allowed us to predict and visualize the possible structural alterations upon disrupting the disulfide bridge. We believe that disrupting the disulfide bridge, which holds the extra fragment loop 2 close to the upper loop, results in the release of the extra fragment loop 2, which fluctuation between the upper loop and the lower loop (extra fragment loop 1) affects cyt c_1 functionality, showed by lower enzyme activity due to the slower electron transfer between cyt c_1 and cyt c, and lower cyt bc_1 complex stability, showed by lower Tm values.

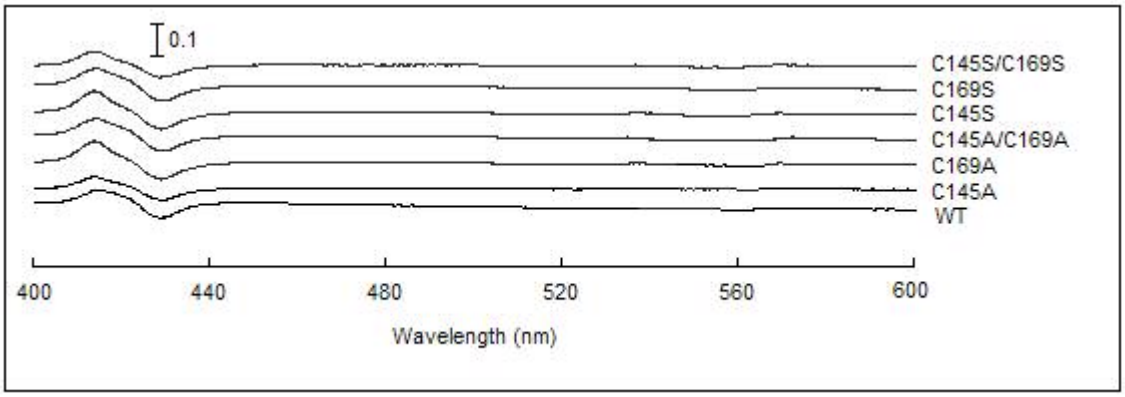

Figure 6: Carbon monoxide optical difference spectra of the cyt bc_1 complexes isolated from wild type and each of the single and double alanine and serine mutants. Carbon monoxide binding was analyzed based on the calculation from (specR+CO) *minus* (specR) as described in materials and methods.

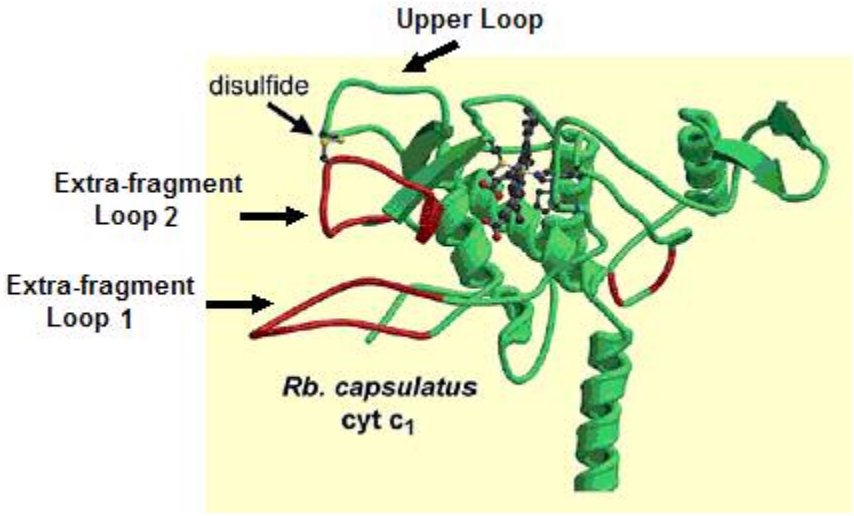

Figure 7: The structure of *Rb. capsulatus* cyt c_1 as reported by Berry, E. et. al. (26) used as a model to predict the structural effect of cystein mutations in *Rb. sphaeroides* cyt c_1. The disulfide bond between the two cysteins is labeled "disulfide". The two long extra-fragment loops present in both *Rb. capsulatus* and *Rhodobacter sphaeroides* cyt c_1 are labeled extra-fragment loop 1 and loop 2 in this figure. The upper loop contains the first cystein (C145 in *Rb. sphaeroides* and C144 in *Rb. capsulatus*).

C. Effect of cystein mutation on the midpoint potential of cytochrome c_1

Mutating the cysteins significantly affects the redox potential of cyt c_1 by lowering it from 230 mV in wild type to as low as 59mV and 48mV in each of the alanine and serine mutants, respectively (Fig. 8, Table 3).

The decrease in midpoint potential explains why cyt c_1 is not fully reducible by ascorbate in any of the cystein mutants (Table 3). Only around 40% and 25% of cyt c_1 is reduced by ascorbate in the alanine and serine mutants, respectively. However, dithionite can reduce all cytochrome c_1 found in solution similar to wild type and cytochrome *b* as well (Fig. 9).

The structural analysis discussed above explains the drop in midpoint potential and therefore the change in ascorbate reducibility. In some proteins, the extra-fragment loop folds close to its native position in wild type protein resulting in a percentage of the population - 40% in alanine mutants and 25% in serine mutants (Fig. 9) - to be reducable by ascorbate. In other proteins, the extra-fragment loop is dislocated farther from its original position, especially upon insertion of a serine residue which causes increased repulsion, resulting in a decrease in cyt c_1 midpoint potential below its ability to be reduced by ascorbate. Clearly, the drop in midpoint potential is not caused by the alteration of any of the heme ligands since none of the mutants binds carbon monoxide but is most likely caused by the structural modification caused by loosening the extra fragment loop affecting the structural integrity around the heme. The decrease in redox potential makes cyt c_1 not fully reducible by ascorbate but fully reducable by dithionite, which midpoint potential is lower than the measured midpoint potential of cyt c_1 mutants.

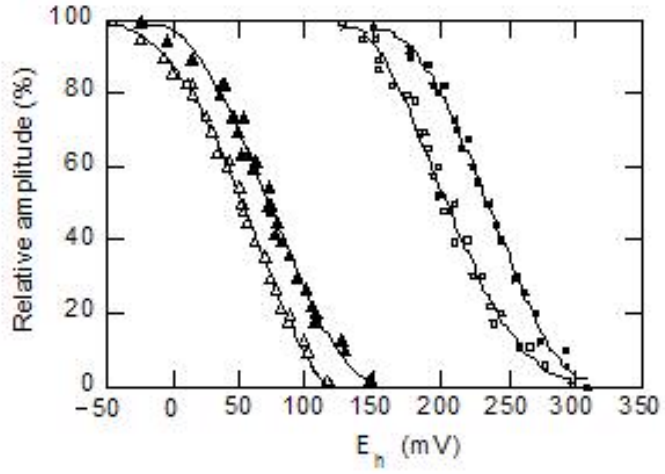

Figure 8: Potentiometric titration of cytochrome c_1 in purified cytochrome bc_1 complexes from Wild type, P151I/F154R and one of each of the cystein mutants to alanine and serine. Plots legend: [▫] Wild type (Em = 235mV), [▪] P151I/F154R (Em = 210mV), [▲] C145A (Em = 64mV) and [△] C145S (Em = 48mV). The Em values for C169A, C145A/C169A, C169S and C145S/C169S mutants are listed in Table 2. Oxidative and reductive titrations were performed as described in Materials and Methods. The data were fit to the Nernst equation for n=1.

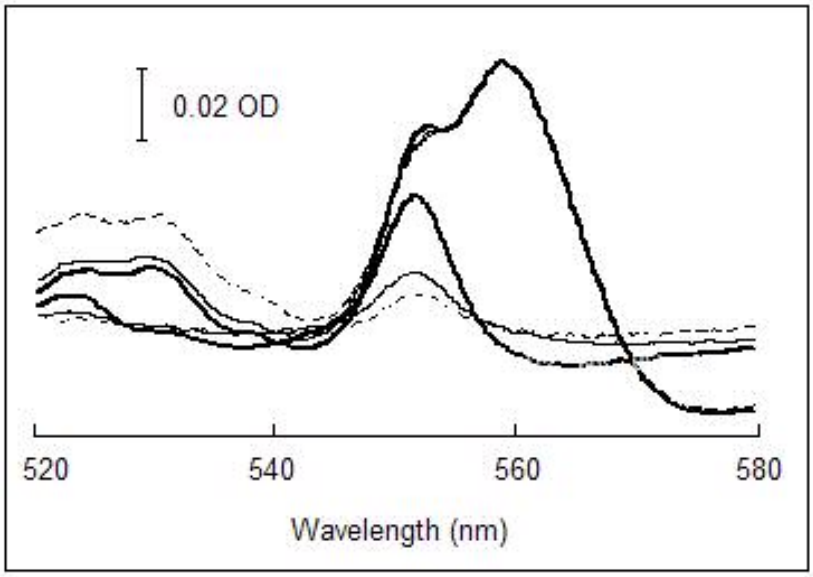

Figure 9: Optical spectral properties of Wild type (thick solid lines), single and double alanine mutants (thin solid lines) and serine mutants (dashed lines). Cytochrome c_1 (553nm) and cytochrome *b* (560nm) concentrations are measured as described in Materials and Methods. Percentage values corresponding to each spectrum are listed in Table 3.

Strain	Enzymatic Activity	% cyt c_1 reduced by Asc	Em (mV)
Wild Type	2.5	100	235
C145A	2.0	40	64
C169A	2.0	40	62
C145A/C169A	2.0	40	59
C145S	1.5	25	48
C169S	1.5	25	49
C145S/C169S	1.5	25	51

Table 3: Redox properties of wild type and mutants of cytochrome c_1 of the cytochrome bc_1 complex. Enzyme activity (specific activity) is expressed as μmol cyt c_{red}/min/nmoles cyt *b*. Midpoint potential (Em) was measured as described in Materials and Methods.

D. Factor Xa digestion of cytochrome c_1

If the disulfide bond exists, cleaving cyt c_1 protein (33KD) between the two cysteins will generate two polypeptides linked through the disulfide bond. Therefore, when the product is run on SDS-PAGE under non-reducing condition, the product will show a similar profile to the undigested protein (33KDa band). However, under reducing conditions where β-mercaptoethanol is used to reduce the disulfide bond, the two peptides will be separated on SDS-PAGE. This approach is valid only if the cleavage site is specific and unique in the protein. Because the amino acid sequence of cyt c_1 does not contain a unique site between the two cysteins, the sequence was screened for the closest match compared to different cleavage enzyme consensus sequence. At position 151-154, a PDGF sequence was mutated to an IDGR sequence, by generating the mutations P151I and F154R simultaneously to match Factor Xa cleavage consensus sequence (IDGR) (Fig.10). P151I/F154R double mutant proteins were purified and characterized and results observed are summarized in Table 4. Mutant cells grow photosynthetically at a same rate than wild type and the specific activity of purified protein is also comparable to wild type. The midpoint potential of cyt c_1 double mutant was measured and determined to be 210mV (Fig. 8, Table 4) compared to wild type cyt c_1 midpoint potential of 235mV. Since the P151I/F154R mutant has similar features to wild type, it is believed to have similar structural folding and can be used to test the presence of disulfide bond in native proteins. Results shown in Fig. 11 reveal that the two fragments remain linked under non-reducing conditions and separate into two fragments of 18KDa and 15KDa, which

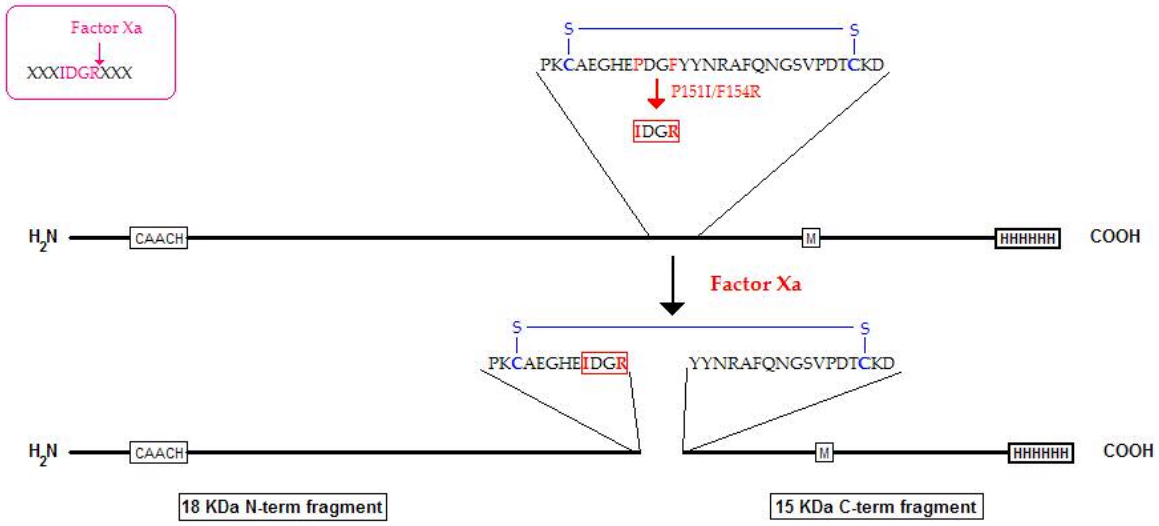

Figure 10: A simplified scheme representing Factor Xa digestion of cyt c_1. The PDGF sequence between the two non heme binding cysteins, C145 and C169, in cytochrome c_1 was mutated to IDGR, Factor Xa consensus sequence. When the protein is treated with Factor Xa, it is cut into two pieces which can only be connected through a disulfide bridge.

Strain	Ps. Growth	Enzymatic activity	Tm (ºC)	% cyt c_1 reduced by Asc	Em (mV)	Cyt c_1 CO binding
Wild Type	+++	2.5	45.2	100	235	-
P151I/F154R	+++	2.5	44.9	100	210	-

Table 4: Characteristics of wild type and P151I/F154R mutant cytochrome c_1 of the cytochrome bc_1 complex. Ps. Growth (+++) represents wild type growth behavior. Enzyme activity (specific activity) is expressed as μmol cyt c_{red}/min/nmoles cyt *b*. Em is the midpoint potential of cytochrome c_1 and Tm is the melting temperature of the cytochrome bc_1 complex, each measured as described in Materials and Methods section.

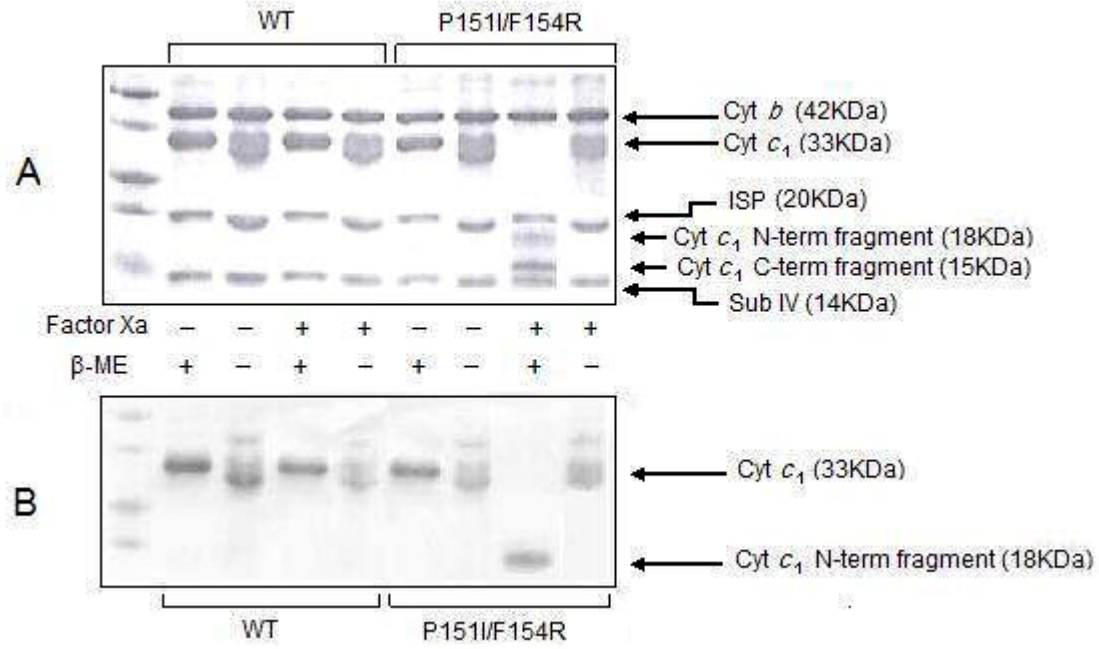

Figure 11: SDS-PAGE analysis and TMBZ heme staining of factor Xa cleavage of the cytochrome bc_1 complex of wild type and P151I /F154R mutant. (A) SDS-PAGE profile of undigested (- Factor Xa) and digested (+ Factor Xa) wild type and Factor Xa cleavable mutant (P151I/F154R) cytochrome bc_1 complex in the presence (+ β-ME) and absence (- β-ME) of reducing agent. Because Factor Xa cleavage site is absent in wild type protein, cyt c_1 remains intact when the protein is digested.

(B) Heme-containing fragments were stained with TMBZ to further confirm the identity of each fragment. Western Blot against His-tag was performed to confirm the identity of the C-terminus fragment (results not shown).

represents the N- terminal fragment containing the heme group (Fig 11. Panel B) and the C-terminal fragment, respectively. These results confirm that the two non-heme binding cysteins in *Rb. sphaeroides* cyt c_1 form a disulfide bridge.

E. Conclusion

The structure *of Rb. sphaeroides* cytochrome bc_1 complex has not been solved yet. The lack of structural data limits proper visualization of the orientation of insertions in the bacterial system. Molecular and biochemical techniques used in this study, with some insight from the structure of *Rhodobacter capsulatus* cytochrome bc_1 complex allowed identification of the orientation, the state and the function of the cysteins, C145 and C169, in *Rhodobacter sphaeroides* cytochrome c_1. The two cysteins where found to be connected through a disulfide bridge which holds the extra-fragment loop 2, containing C169, in a fixed position close to the upper loop, containing C145. Ile183 of the βXM motif does not seem to be correlated to the presence of the disulfide bridge since no revertants were observed.

Disruption of the disulfide bridge seems to result in the release of the second extra fragment loop, which fluctuation slows the cytochrome bc_1 complex activity and significantly lowers its stability and the redox potential of cytochrome c_1.

REFERENCES

1. Hauska, G., Hurt, E., Gabellini, N., and Lockau, W. (1983) Comparative aspects of quinol-cytochrome *c* - plastocyanin oxidoreductases. *Biochim. Biophys. Acta* **726**, 97-133

2. Hatefi, Y. (1985) The mitochondrial electron transport and oxidative phosphorylation system. *Annu Rev Biochem* **54**, 1015-1069

3. Trumpower, B. L. (1990) Cytochrome bc_1 complexes of microorganisms *Microbiol. Rev.* **54**, 101-129

4. Trumpower, B.L., and Gennis R. B. (1994) Energy transduction by cytochrome complexes in mitochondrial and bacterial respiration: the enzymology of coupling electron transfer reactions to transmembrane proton translocation. *Annu. Rev. Biochem.* **63**, 675-716

5. Berry, E. A., Guergova-Kuras, M., Huang, L. S., and Crofts, A. R. (2000) Structure and function of cytochrome *bc* complexes. *Annual Rev. Biochem.* **69**, 1005-1075

6. Schagger, H., Brandt, U., Gencic, S., and Von Jagow, G. (1995) Ubiquinol-cytochrome *c* reductase from human and bovine mitochondria. *Methods Enzymol.* **260**, 82-96

7. Ljungdahl, P. O., Pennoyer, J. D., Robertson, D. E., and Trumpower, B. L. (1987) Purification of highly active cytochrome bc_1 complexes from phylogenetically

diverse species by a single chromatographic procedure. *Biochim. Biophys. Acta* **891**, 227-241

8. Yu, L., Tso, S. C., Shenoy, S.K., Quinn, B. N., and Xia, D. (1999) The role of the supernumerary subunit of Rhodobacter sphaeroides cytochrome bc_1 complex. *J. Bioenerg. Biomembr.* **31**, 251-257

9. Robertson, D. E., Ding, H., Chelminski, P. R., Slaughter, C., Hsu, J., Moomaw, C., Tokito, M., Daldal, F., and Dutton, P. L. (1993) Hydroubiquinone-cytochrome c_2 oxidoreductase from *Rhodobacter capsulatus*: definition of a minimal, functional isolated preparation. *Biochemistry* **32**, 1310-1317

10. Yu, L., Tso, S. C., Shenoy, S. K., Quinn, B. N., and Xia, D. (1999) The role of the supernumerary subunit of *Rhodobacter sphaeroides* cytochrome bc_1 complex. *J. Bioenerg. Biomembr.* **3**, 251-257. Review

11. Mitchell, P. (1976) Possible molecular mechanisms of the protonmotive function of cytochrome systems. *J Theor Biol* **62**, 327-367

12. Crofts, A. R., Shinkarev, V. P., Kolling, D. R., and Hong, S. (2003) The modified Q-cycle explains the apparent mismatch between the kinetics of reduction of cytochromes c_1 and b_H in the bc_1 complex. *J Biol Chem*. **278**, 36191-36201

13. Trumpower, B. L. (1990) The protonmotive Q cycle. Energy transduction by coupling of proton translocation to electron transfer by the cytochrome bc_1 complex. *J Biol Chem* **265**, 11409-11412

14. Gao, X., Wen, X., Yu, C., Esser, L., Tso, S., Quinn, B., Zhang, L., Yu, L., and Xia, D. (2002) The crystal structure of mitochondrial cytochrome bc_1 in complex with

famoxadone: the role of aromatic-aromatic interaction in inhibition. *Biochemistry* **41**, 11692-11702

15. Zhang, Z., Huang, L., Shulmeister, V. M., Chi, Y. I., Kim, K. K., Hung, L. W., Crofts, A. R., Berry, E. A., and Kim, S. H. (1998) Electron transfer by domain movement in cytochrome bc_1. *Natur*e **392**, 677-684

16. Hunte, C., Koepke, J., Lange, C., Rossmanith, T., and Michel, H. (2000) Structure at 2.3 A resolution of the cytochrome bc_1 complex from the yeast Saccharomyces cerevisiae co-crystallized with an antibody Fv fragment . *Structure Fold Des* **8**, 669-684

17. Yu, C. A., Xia, J. Z., Kachurin, A. M., Yu, L., Xia, D., Kim, H., and Deisenhofer, J. (1996) Crystallization and preliminary structure of beef heart mitochondrial cytochrome bc_1 complex. *Biochim Biophys Acta* **1275**,47-53. Review

18. Xiao, K., Chandrasekaran, A., Yu, L., and Yu, C. A. (2001) Evidence for the intertwined dimer of the cytochrome bc_1 complex in solution. *J Biol Chem* **276**, 46125-46131

19. Gong, X., Yu, L., Xia, D., and Yu, C. A. (2005) Evidence of electron equilibrium between the two hemes b_L in the dimeric cytochrome bc_1 complex. *J. Biol. Chem*. **280**, 9251-9257

20. Kim, H., Xia, D., Yu, C.A., Xia, J. Z., Kachurin, A. M., Zhang, L., Yu, L., ND Deisenhofer, J. (1998) Inhibitor binding changes domain mobility in the iron-sulfur protein of the mitochondrial bc_1 complex from bovine heart. *Proc Natl Acad Sci USA* **95**, 8026-8033

21. Gao, X., Wen, X., Esser, L., Quinn, B., Yu, L., Yu, CA., and Xia, D. (2003) Structural basis for the quinone reduction in the bc_1 complex: a comparative analysis of crystal structures of mitochondrial cytochrome bc_1 with bound substrate and inhibitors at the Qi site. *Biochemistry* **42**, 9067-80

22. Esser, L., Quinn, B., Li, Y.F., Zhang, M., Elberry, M., Yu, L., Yu, C.A., and Xia, D. (2004) Crystallographic studies of quinol oxidation site inhibitors: a modified classification of inhibitors for the cytochrome bc_1 complex. *J Mol Biol*. **341**, 281-302.

23. Tian, H., Yu, L., Mather, M. W., and Yu, C. A. (1998) Flexibility of the neck region of the rieske iron-sulfur protein is functionally important in the cytochrome bc_1 complex. *J. Biol. Chem*. **273**, 27953-27959

24. Tian, H., White, S., Yu, L., and Yu, C.A. (1999) Evidence for the head domain movement of the rieske iron-sulfur protein in electron transfer reaction of the cytochrome bc_1 complex. *J. Biol. Chem*. 274, 7146-7152

25. Xiao, K., Yu, L., and Yu, C. A. (2000) Confirmation of the involvement of protein domain movement during the catalytic cycle of the cytochrome bc_1 complex by the formation of an intersubunit disulfide bond between cytochrome *b* and the iron-sulfur protein. *J. Biol. Chem*. **275**, 38597-38604

26. Kim, H., Xia, D., Yu, C.A., Xia, J. Z., Kachurin, A. M., Zhang, L., Yu, L., and Deisenhofer, J. (1998) Inhibitor binding changes domain mobility in the iron-sulfur protein of the mitochondrial bc_1 complex from bovine heart. *Proc Natl Acad Sci USA* **95**, 8026-8033

27. Yu CA, Tian H, Zhang L, Deng KP, Shenoy SK, Yu L, Xia D, Kim H, and Deisenhofer J. (1999) Structural basis of multifunctional bovine mitochondrial cytochrome bc_1 complex. *J. Bioenerg Biomembr.* **3**,191-199. Review

28. Yakushiji, E., Okunuki, K., (1940) Mitochondrial cytochrome c_1. *Imp. Acad*. Tokyo **16**, 299-305

29. Keilin, D., Hartree, E. F., (1940) Mitochondrial cytochrome c_1. *Proc. R. Soc. London Ser. B.* **129**, 277-283

30. Wakabayashi, S., Matsubara, H., Kim, C.H., Kawai, K., and King, T.E. (1980) The complete amino acid sequence of bovine heart cytochrome c_1. *Biochem. Biophys. Res. Commun.* **97**, 1548-1554

31. Gonzales, D.H., and Neupert, W. (1990) Biogenesis of mitochondrial c-type cytochromes. *J. Bioenerg. Biomembr*. **22**, 753-768

32. Yun, C.H., Beci, R., Crofts, A.R., Kaplan, S., and Gennis, R.B. (1990) Cloning and DNA sequencing of the *fbc* operon encoding the cytochrome bc_1 complex from *Rhodobacter sphaeroides*. Characterization of *fbc* deletion mutants and complementation by a site-specific mutational variant. *Eur J Biochem.* **194**, 399-411.

33. Lange, C., and Hunte, C. (2002) Crystal structure of the yeast cytochrome bc_1 complex with its bound substrate cytochrome *c*. *Proc. Natl. Acad. Sci.* **99**, 2800–2805

34. Xia, D., Yu, C. A., Kim, H., Xia, J. Z., Kachurin, A. M., Zhang, L., Yu, L., and Deinsenhofer, J. (1997) Crystal structure of the cytochrome bc_1 complex from bovine heart mitochondria. *Science* **277**, 60–66.

35. Zhang, Z., Huang, L., Shulmeister, V. M., Chi, Y., Kim, K. K., Hung, L., Crofts, A. R., Berry, E. A., and Kim, S. (1998) Electron transfer by domain movement in cytochrome bc_1. *Nature* **392**, 677–684.

36. Iwata, S., Lee, J.W., Okada, K., Lee, J.K., Iwata, M., Rasmussen,B., Link, T.A., Ramaswamy, S., and Jap, B.K. (1998) Complete structure of the 11-subunit bovine mitochondrial cytochrome bc_1 complex. *Science* **281**, 64–71

37. Osyczka, A., Dutton, P. L., Moser, C. C., Darrouzet, E., and Daldal. F. (2001) Controlling the functionality of cytochrome c_1 redox potentials in the *Rhodobacter capsulatus* bc_1 complex through disulfide anchoring of a loop and a β-branched anmino acid near the heme-ligating methionine. *Biochemistry* **40**:14547-56.

38. Berry, E.A., Huang, L.S., Saechao, L. K., Ning, G.P., Valkova-Valchanova, M., and Daldal, F. (2004) X-ray structure of *Rhdobacter capsulatus* cytochrome bc_1: comparison with its mitochondrial and chloroplast counterparts. *Photosynthesis research* **81**, 251-275

39. Yu, C. A., and Yu, L. (1982) Synthesis of biologically active ubiquinone derivatives. *Biochemistry* **21**, 4096-4101

40. Yu, C. A., Chiang, Y. L., Yu, L., and King, T. E. (1975) Photoreduction of cytochrome c_1. *J. Biol. Chem*. **250**, 6218-6221

41. Mather, M. W., Yu, L., and Yu, C. A. (1995) The involvement of threonine 160 of cytochrome *b* of *Rhodobacter sphaeroides* cytochrome bc_1 complex in quinone binding and interaction with subunit IV. *J. Biol. Chem*. **270**, 28668-28675

42. Tian, H., Yu, L., Mather, M. W., and Yu, C. A. (1997) The involvement of serine 175 and alanine 185 of cytochrome *b* of *Rhodobacter sphaeroides* cytochrome bc_1 complex in interaction with iron-sulfur protein. *J. Biol. Chem*. **272**, 23722-23728

43. Berden, J. A., and Slater, E. C. (1970) The reaction of antimycin with a cytochrome *b* preparation active in reconstitution of the respiratory chain. *Biochim. Biophys. Acta* **216**, 237-249

44. Yu, L., Dong, J. H., and Yu, C. A. (1986) Characterization of purified cytochrome c_1 from *Rhodobacter sphaeroides* R-26. *Biochim. Biophys. Acta* **852**, 203-211

45. Laemmli, U. K. (1970) Cleavage of structural proteins during the assembly of the head of bacteriophage T4. *Nature* **227**, 680-685

46. Dutton, P. L. (1978) Redox potentiometry: determination of midpoint potentials of oxidation-reduction components of biological electron-transfer systems. *Methods Enzymol*. **54**, 411-435

47. Guner, S., Robertson, D. E., Yu, L., Qiu, Z. H., Yu, C. A., and Knaff, D. B. (1991) The *Rhodospirillum rubrum* cytochrome bc_1 complex: redox properties, inhibitor sensitivity and proton pumping. *Biochim. Biophys. Acta* **1058**, 269-279

48. Konishi, K., Van Doren, S. R., Kramer, D. M., Crofts, A. R., and Gennis, R. B. (1991) Preparation and characterization of the water-soluble heme-binding domain of cytochrome c_1 from the *Rhodobacter sphaeroides* bc_1 complex. *J. Biol. Chem.* **266**, 14270-14276

49. Qi, P. X., Di Stefano, D. L., and Wand, A. J., (1994) Solution structure of horse heart ferrocytochrome *c* determined by high-resolution NMR and restrained simulated annealing. *Biochemistry* **33**, 6408-6417

50. Xia, D., Yu, C. A., Kim, H., Xia, J. Z., Kachurin, A. M., Zhang, L., Yu, L., and Deisenhofer, J. (1997) Crystal structure of the cytochrome bc_1 complex from bovine heart mitochondria. *Science* **277**, 60-66.

VITA

Maria Elberry

Candidate for the Degree of

Master of Science

Thesis: STUDIES OF THE CYTOCHROME c_1 SUBUNIT OF THE CYTOCHROME bc_1 COMPLEX FROM *RHODOBACTER SPHAEROIDES*

Major Field: Biochemistry and Molecular Biology

Biographical:

Personal Data: Born in Ghosta, Lebanon, on October 29, 1981. Proud Daughter of Antoine Elberry and Joumana Saber.

Education: Graduated from Saint Coeurs-Kfarahbab High school in June 1999; Received Bachelor Degree in Biology from Lebanese American University, Byblos, Lebanon, in June 2002. Completed requirements for the Masters of Science degree at Oklahoma State University in Dec 2005.

Name: Maria Elberry Date of Degree: December 2005
Institution: Oklahoma State University Location: Stillwater

Title of Study: STUDIES OF THE CYTOCHROME c_1 SUBUNIT OF THE CYTOCHROME bc_1 COMPLEX FROM *RHODOBACTER SPHAEROIDES*

Pages in Study: 47 Candidate for the Degree of Master of Science

Major Field: Biochemistry and Molecular Biology

Scope and Method of Study: Determine the state of the two non-heme binding cysteins in cytochrome c_1 head domain of the cytochrome bc_1 complex from *Rhodobacter sphaeroides* using genetic and biochemical techniques.

Findings and Conclusions: The cytochrome c_1 of *Rhodobacter sphaeroides* bc_1 complex contains several insertions and deletions that distinguish it from the complex of other higher organisms. Additionally, it contains two non-conserved cysteins, C145 and C169. The orientation of the insertions and the state of these non-heme binding cysteins remain unknown. Mutating one or both cysteins is found to have comparable effects on the functionality of the cytochrome bc_1 complex. Mutants show decreased activity but can still support a delayed photosynthetic growth. The mutated cytochrome c_1 has a decreased Em, without any alteration in the heme ligation environment, caused by a structural modification in the head domain of cytochrome c_1. Analysis of the mutants reveals that the two cysteins form a disulfide bridge. Cleavage of cytochrome c_1 between the two cysteins followed by gel electrophoresis show two fragments only under reducing conditions confirming the existence of a disulfide bridge. The disulfide bridge is essential in maintaining the structural integrity of cytochrome c_1 and thus the functionality of the cytochrome bc_1 complex.

ADVISER'S APPROVAL: Dr. Chang-An Yu